

# A Cooperative Advanced Driver Assistance System to Mitigate Vehicular Traffic Shock Waves

Markus Forster\*, Raphael Frank\*, Mario Gerla<sup>†</sup> and Thomas Engel\*

\*Interdisciplinary Centre for Security, Reliability and Trust,

University of Luxembourg, 1359, Luxembourg

{ markus.forster|raphael.frank|thomas.engel }@uni.lu

<sup>†</sup>Dept. of Computer Science, UCLA, CA 90095, USA

gerla@cs.ucla.edu

**Abstract**—We address the problem of shock wave formation in uncoordinated highway traffic. First, we identify the combination of heavy traffic and small traffic perturbations or unexpected driver actions as the main causes of highway traffic jams. Then we introduce a novel distributed communication protocol that enables us to eliminate upstream shock wave formation even with low system penetration rates. Based on traffic information ahead, we propose a *Cooperative Advanced Driver Assistance System* (CADAS) that recommends non-intuitive velocity reductions in order to redistribute traffic more uniformly thereby eliminating traffic peaks. Simulation results show that CADAS significantly increases the average velocity and therewith reduces the overall travel time and avoids unnecessary slowdowns.

**Keywords**— *Traffic Modeling, Vehicular Networks, Congested Flow, Shock Waves*

## I. INTRODUCTION

Traffic demand on major highways and freeways has increased significantly over recent decades. To address the problem of vastly rising traffic volume the traditional solution has been the extension of the road network by constructing new highways or adding lanes to already existing ones. This strategy however has reached a point where in most areas physical road extensions are no longer possible [1]. As a possible remedy, one should also consider the fact that, due to current completely uncoordinated vehicular traffic, the highway capacity is not fully exploited. Simulations and empirical analysis have shown that vehicular traffic is in *free flow* mode only for relatively low densities when interactions between vehicles are negligible [2]. Maximum lane capacity is reached for a density between 13 vehicles per kilometer and 17 vehicles per kilometer [3]–[6].

To overcome this situation it is necessary to exploit modern *Intelligent Transportation Systems* (ITS) technology that equips vehicles with several sensors, enabling them to recognize their surroundings and to notify motorists to take corrective actions or, in some cases, to implement such corrections automatically. Many of the *Advanced Driver Assistance Systems* (ADAS) are already implemented in luxury class vehicles to improve safety and driver comfort. An example of such a system is the *Adaptive Cruise Control* (ACC) System that can maintain minimum safety headway to the vehicle ahead. Such systems can react much faster than the human to abrupt downstream vehicle maneuvers and therefore allow to use smaller safety distances [7]. Studies have already shown

that setting speed limits on highways with high traffic demand, as can be done with ADAS and with properly spaced road advisory panels, can increase overall traffic flow [8]. One unfortunate limitation of such systems is drivers' or sensors' line of sight. Moreover, such a system can improve the overall situation only with full ADAS coverage of the entire road fleet in order to guarantee collision-free driving with smaller headways.

In this paper we introduce a novel approach for a *Cooperative Advanced Driver Assistance System* (CADAS) that connects vehicles via *Vehicular ad hoc Networks* (VANETs) and lets them exchange recent and relevant traffic information. The proposed protocol, *Density Redistribution through Intelligent Velocity Estimation* (DRIVE), broadcasts critical information such as slowdowns. This information can be used by following vehicles far behind to learn about the traffic situation downstream. This information is collected and evaluated in a way that provides a consistent picture of the traffic situation ahead. By using the well-known *Lighthill-Whitham-Richard model* (LWR) [3], [4], it is possible to estimate a density gradient between two communicating vehicles and use this information for velocity estimations. The aim of this protocol is to redistribute oncoming vehicles in a way that prevents congestion shock waves from forming. We show that, by giving individual velocity prescriptions, even with a low number of participants one can achieve significant improvements in overall traffic flow and average travel times. Since this does not lead to a reduction in safety distance, full system coverage is not required to ensure collision-free driving.

The remainder of this paper is organized as follows: In Section 2 we give a brief problem statement, followed by a description of the two well-established traffic models used in this paper in Section 3. In Section 4 we introduce DRIVE, our novel protocol for traffic flow optimization. An evaluation is given in Section 5. In Section 6 an overview of related work is provided. Finally a conclusion is drawn in Section 7.

## II. PROBLEM STATEMENT

In this section we provide a brief introduction to the mechanisms of shock wave emergence and give an initial proposal for solving the problem of the appearance of undesirable traffic formations with the help of modern inter-vehicular communication mechanisms. The main cause for the formation of shock waves is the combination of high traffic demand and

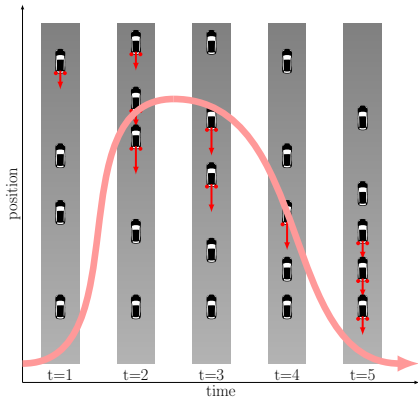


Fig. 1: Formation of a shock wave stream upwards

unexpected driver actions. This means that, in dense traffic situations, even a minor flaw in driver behavior or traffic even along the path can create a temporary overload that leads to the formation of a shock wave upward in the traffic stream. Examples of physical perturbations are ramps, construction sites, a simple increase in traffic or reduction of lanes. Beyond that, small driving imperfections like the human tendency to delayed reaction can cause flow disruptions, leading to congestion [9], [10].

Figure 1 demonstrates the formation of a shock wave in a simple one-lane road scenario. From left to right the graph depicts the same road segment at consecutive time steps. In the first time step, the leading vehicle slows down for some unknown reason, as depicted by the red arrow against the driving direction. In the next time step the vehicles that follow must adapt their speeds in order not to crash into the lead vehicle. Hence, the new velocity of the following vehicles must be decreased below that of the leading one. During the following time steps, this prescription to brake travels upstream forming a shock wave. *Stop-and-Go* traffic often seems to appear out of nowhere and the resulting congestions are often referred to as *phantom jams*. For more information we direct the reader to [11], [12].

As one can see in Figure 1, vehicles are not able to react until the incident that triggered the wave is in line of sight. This means that hard braking maneuvers are necessary to avoid a crash. Afterwards the motorists have to accelerate again when leaving the congested area. This implies a waste of energy and an increase in emissions.

Due to the fact that traffic density on a sufficiently long road segment is not uniformly distributed, one can experience clusters with high density and intermediate sections with lower densities. Our work takes advantage of this phenomenon. Communication between vehicles enables us to exchange relevant information over long distances, extending the awareness horizon of the vehicle. Having the information available over long distances upstream in the traffic flow gives us the opportunity to react to the traffic situation ahead with more foresight than without communication [13].

### III. TRAFFIC MODELS

To implement, test and verify new strategies for traffic flow optimization it is necessary to have a well-established model of traffic dynamics in the first place. It is fundamental

to have a mathematical abstraction that has been proven to accord with empirical data, measured in real traffic so as to have evidence that the simulated results are comparable to the empirical ones. In the simulation of traffic dynamics two main classes of traffic models have to be distinguished, namely *macroscopic* and *microscopic* models. For our studies we need both: a *microscopic* model to simulate each distinct vehicle in real time, and a *macroscopic* model to estimate the traffic situation between two communicating vehicles. A brief classification of the different models is given in the following paragraphs.

**Macroscopic models:** *Macroscopic models* describe the observable traffic flow on a road segment by analogy with the physical equations for fluid dynamics. They give an overview of the general traffic situation without distinction between single vehicles. The observable values for this class of models are the vehicular density  $\rho(x, t)$ , the traffic flow  $Q(x, t)$  and the mean velocity  $V(x, t)$ , observed within a given road segment. The base equation for those models is the flow equation:

$$Q(x, t) = \rho(x, t) \cdot V(x, t) \quad (1)$$

Typically, those parameters can be measured with *loop detectors* or with the less common *radar detectors* or *visual detectors*. Obviously, it is easy to measure the flow as the number of vehicles  $N$  that pass the detector within a given time  $T$ . Additionally, most detectors are able to measure the velocity of the passing vehicles, giving the mean velocity by summing up single velocities  $v_i; i \in \mathbf{I}$ , where  $\mathbf{I}$  is an index set, and dividing the sum by the number of passing vehicles  $N$ . In mathematical notation this means:

$$Q(x) = \frac{N}{T} \quad (2)$$

$$V(x) = \frac{1}{N} \sum_{i=1}^N v_i \quad (3)$$

**Microscopic models:** The second class of traffic models consists of the *microscopic models*, which describe the reaction of each distinct vehicle with respect to its neighbors. The observed values are position, velocity and acceleration.

The two traffic models used within this paper are the well-established *Krauss model* for microscopic traffic simulation of the vehicles on the observed road and the LWR model for the estimation of shock wave propagation upstream in the macroscopic traffic flow. They are introduced in the following paragraphs.

#### A. Krauss car-following model

The car-following model, introduced by Krauss [14], [15] is time-discrete and continuous in space, meaning that while the model states are evaluated for a distinct time step, the space is not divided into distinct cells. The model belongs to the class of *microscopic traffic models*, implying that it describes the behavior of each single vehicle.

The model is strongly related to *Cellular Automata* (CA) models introduced by Nagel and Schreckenberg [10], [16] but it extends them using more realistic acceleration  $a_i(v)$  and deceleration  $b_i(v)$  behavior. Furthermore, a parameter for the vehicle length is introduced to allow the possibility of different vehicle classes on the simulated road. The spatial continuity

is another difference from the CA models. It allows vehicles to be positioned at any location on the given road segment instead of in discrete cells, as given with the CA models.

In each simulation step, the following three rules are applied to each distinct vehicle on the observed road segment:

*a) Velocity Update:* The velocity update phase determines the new velocity by taking the minimum value among the maximal allowed velocity, the safety velocity and the desired velocity as given by equation:

$$v_i(t+1)^{(1)} = \min[v_{\max}, v_i(t) + a_i(v_i(t))\Delta t, v_{i,\text{safe}}(t)] \quad (4)$$

This minimum ensures that the computed velocity is always valid with respect to collision avoidance. The safety velocity  $v_{\text{safe}}$  is calculated by the formula:

$$v_{i,\text{safe}}(t) = v_{i-1}(t) + b_i(v_i(t)) \frac{g_i(t) - v_{i-1}(t)}{v_i(t) + b_i(v_i(t))} \quad (5)$$

with  $g_i(t) = x_{i-1}(t) - x_i(t) - 1$ , the gap between vehicles  $i-1$  and  $i$ ,  $x_{i-1}(t)$  the position and  $v_{i-1}(t)$  the velocity of the preceding vehicle, respectively.

*b) Randomization:* In the *randomization phase* a probabilistic tendency for human inaccuracy is applied to the velocity computation. This is necessary to extend the fully-deterministic modeling of the *velocity update* to simulate velocity differences and consequent emergence of *phantom jams*. Moreover, this gives a much more realistic description of real traffic on highways. The following equations apply this probabilistic factor to the deterministic model:

$$v_i(t+1)^{(2)} = \begin{cases} v_i(t+1)^{(1)} - b\Delta t & \text{with } P_d(v(t)) \\ v_i(t+1)^{(1)} & \text{else} \end{cases} \quad (6)$$

where

$$P_d(v(t)) := \begin{cases} p_s & \text{if } v(t) = 0 \\ p_m & \text{else} \end{cases} \quad (7)$$

with  $p_m$  the probability of dallying for moving vehicles and  $p_s$  the one for standing vehicles, respectively. It holds true that  $p_m \ll p_s$ . Equation 6 causes vehicle  $i$  to reduce its velocity by a deceleration  $b$  for one time step with a velocity-dependent probability  $P_d(v(t))$ .

Finally, the maximum of this newly-computed velocity and zero is taken to ensure that velocities are never negative:

$$v_i(t+1) = \max[0, v_i(t+1)^{(2)}] \quad (8)$$

Hence, the velocity of vehicle  $i$  for the actual step is computed by a deterministic acceleration rule as well as a probabilistic dally factor.

*c) Position Update:* The final step for each vehicle per simulation round is the processing of its movement. The new position is computed by the addition of the old position and the new velocity multiplied by the constant time difference  $\Delta t$  as given in the following:

$$x_i(t+1) = x_i(t) + v_i(t+1)\Delta t \quad (9)$$

These three rules are applied for each discrete time step of the simulation.

Lane change behavior on multi-lane roads is based on three simple assumptions:

- lane changes are performed if they are safe and favorable
- bypassing on right lane is only allowed within congestion (this is a special case for European Highways)
- to introduce some randomness to the behavior of the driver there exists a small probability for lane change that is safe but not favorable

Please note that in this context *safe* means that the system ensures collision-free driving. For more information on lane changing behavior, we direct the reader to [15].

### B. Lighthill-Whitham-Richards model

The LWR model, introduced by Lighthill and Whitham [3] as well as independently by Richards [4], is based on the continuity equation:

$$\frac{\partial \rho}{\partial t} + \frac{\partial (\rho V)}{\partial x} = 0 \quad (10)$$

The evolution of density over time is given by the spatial evolution of traffic flow. This holds true for homogeneous road segments where inputs and outputs are only possible at the borders of the observed segment. The model states that there exists a static relation between the traffic flow  $Q(x, t)$  and the vehicular density  $\rho(x, t)$  of the form:

$$Q(x, t) = \hat{Q}(\rho(x, t)) \quad (11)$$

By substituting equation 11 into equation 10, we obtain the model equation of the LWR model, given as:

$$\frac{\partial \rho}{\partial t} + \frac{d\hat{Q}(\rho)}{d\rho} \frac{\partial \rho}{\partial x} = 0 \quad (12)$$

Since equation 12 is a *Transport Equation*, substituting the general wave ansatz  $\rho(x, t) = \rho_0(x - \tilde{c}t, t)$  into equation 12 we can rewrite it as:

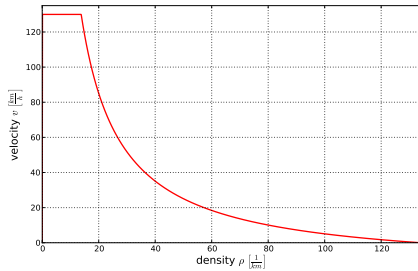
$$v_t + C \cdot v_x = 0 \quad (13)$$

and the solution for the LWR model giving the shock wave's propagation velocity yields:

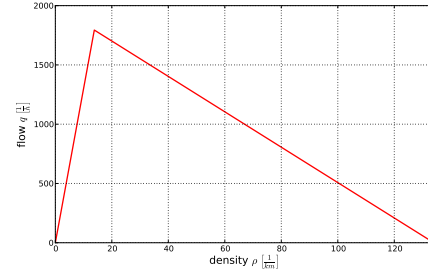
$$\tilde{c} = -\frac{d\hat{Q}(\rho)}{d\rho} \quad (14)$$

For more details, we direct the reader to [3], [4].

This means that the propagation velocity of the shock wave is proportional to the gradient in the flow-density chart. For the triangular flow-density chart depicted in Figure 2b, one can read the propagation velocity of a shock wave directly as the gradient of the flow-density chart if both points of interest are in the same traffic phase. For the *free flow phase* the shock wave travels downwards in the traffic flow with the maximum allowed velocity  $v_{\max}$  and therefore does not affect preceding vehicles. In contrast, in the *congested phase* the propagation velocity becomes negative, hence the shock wave travels upstream in the traffic flow, interacting with the following vehicles with a velocity  $\tilde{c} \approx -15$  km/h, causing slow downs [17].



(a) Velocity Density Chart



(b) Flow Density Chart

Fig. 2: Triangular fundamental properties of a simplified LWR model

#### IV. PROTOCOL DESCRIPTION

In this section we introduce the new communication protocol *Density Redistribution through Intelligent Velocity Estimation* (DRIVE). In a first attempt, a new Vehicle to Vehicle (V2V) communication protocol is introduced to extend the awareness horizon far beyond the line of sight. With our protocol it is possible to anticipate velocities upstream in the traffic flow in order to prevent congestions caused by temporarily increasing vehicular densities. The novelty, introduced in DRIVE is the approach to estimate the traffic conditions in the interspace between two communicating vehicles without knowing the percentage of participants. To fulfill this task, an estimation is drawn by the use of the well established LWR model [3], [4], described in section III-B.

The network protocol proposed in this paper is fully compliant with the IEEE 802.11p standard for *Wireless Access in Vehicular Environments* [18]. Message propagation can be realized by the use of the *Cooperative Awareness Message* [19].

DRIVE is a connectionless and event driven networking protocol, meaning that vehicles broadcast their messages in a burst, only in case of a significant slowdown or if the velocity falls below a given threshold. Each message has a certain Time To Live (TTL) to ensure that it reaches the neighbors that are within transmission range. The strategy is based on three distinct phases, namely the *notification phase*, the *reception phase* and the *forwarding phase*. The aim of the protocol is to redistribute the upstream vehicular density in a way that avoids the formation of a shock wave in case of a temporary peak in traffic demand. Although the communication part of DRIVE is independent from the number of lanes, the recommendation algorithm is lane-based, meaning that only vehicles in the same driving lane will get a velocity recommendation from the system. For lane determination accuracy, we assume that participating vehicles have cruise control with optic sensors that can determine the lane. This behavior is motivated by the assumption that a slowdown recommendation for the left lane while having free-flowing traffic in the right lane will be disregarded by a human driver anyway.

When a slowdown event is detected, the leading vehicle sends a message containing the actual location and vehicle dynamics. The next vehicle in the information chain receives this message, adapts its velocity according to the recommendation by DRIVE, and sends a notification containing its own slowdown information further upstream rebroadcasting

the received message. This chain of messages ends if the system determines that no action has to be taken, there is no vehicle within transmission range to receive a message or if the maximum propagation radius for a distinct message is reached.

In the following subsections, the mechanism of the message exchange and the computation of the anticipated velocity is described in more detail.

##### A. Notification Phase

A vehicle that has to slow down by more than a certain threshold  $\Delta v_n$  or is moving with a velocity lower than the minimum expected ( $v_{\min}$ ) triggers an event and broadcasts a message

$$m_h = [id, x_s, y_s, x_o, y_o, t_o, v_o, v_{o,t-1}] \quad (15)$$

where  $h \in \mathbf{H}$  is a unique message identifier and  $id$  is a unique identification of the originating vehicle.  $x_s$  and  $y_s$  are the GPS-coordinates of the sending vehicle, whereas  $x_o$  and  $y_o$  are the GPS-coordinates of the originator. The remaining values are the timestamp of the originator at message creation ( $t_o$ ), the actual velocity of the originator at message creation ( $v_o$ ) and the velocity of the originator one time step before message creation ( $v_{o,t-1}$ ). All values in the message except for  $id, t_o$  and  $v_{o,t-1}$  are functions of  $t$ . (The indices have been omitted to improve readability.)

##### B. Reception Phase

Every second, the protocol checks all received messages to select the most recent one. The velocity of the messaging vehicle is then compared to the receiver's velocity. If the sender's velocity is lower than the receiver's, the protocol estimates the traffic situation between the source vehicle and the notified one. The DRIVE protocol will then give a velocity recommendation to the motorist to avoid the formation of a shock wave.

A more detailed description of the *reception phase* is given next, together with the mathematical foundation.

Vehicles receiving a message  $m_h$  have to check first if this message is relevant for them. This means that a vehicle  $i$ , receiving a set of messages  $\mathcal{M} = \{\dots, m_h, m_k, m_l, \dots\}; h, k, l \in \mathbf{H}$  has first to find the message  $m_j$  having the least distance to the originator. Explicitly, this means

$$m_j = \min_{m_h \in \mathcal{M}} (\text{dist}(i, m_h)) \quad (16)$$

Hence, message  $m_j$  is considered the most recent information affecting vehicle  $i$  if the spatial distance between vehicle  $i$  and  $j$  is less than that between  $i$  and any other messaging vehicle but not larger than the wavelength of a shock wave, both vehicles are driving in the same direction, vehicle  $j$  is ahead of vehicle  $i$  and both vehicles are driving in the same lane. One other important constraint is that the velocity for the messaging vehicle  $v_t$  is less than  $3/4$  of the maximum allowed velocity  $v_{\max}$  on the observed lane.

In the next step, it is necessary to estimate the traffic situation between the receiving vehicle  $i$  and the sending vehicle  $j$ . To do this, the road segment between vehicle  $i$  and vehicle  $j$  must be considered as homogeneous; that is, equation 10 holds true. This means that it is possible to apply equation 12 and thus to estimate the density gradient in the interval  $[x_i, x_j]$ .

For simplicity, the protocol uses a LWR model with a triangular fundamental diagram and the corresponding velocity density chart, as depicted in Figure 2. This characteristic of the LWR model has some special properties. The model suggests that, in free flow, motorists tend to drive with the maximum possible or allowed velocity  $v_{\max}$ . The critical density, where the traffic turns from free flow to the congested phase, is given by:

$$\rho_k = \frac{1}{v_{\max}T + \left(\frac{1}{\rho_{\max}}\right)} \quad (17)$$

meaning that the optimal spacing between consecutive vehicles is given by the gap needed to drive with maximum velocity  $v_{\max}$  for the minimum time headway  $T$  plus the effective vehicle length  $\frac{1}{\rho_{\max}}$ .

For the LWR model with a triangular fundamental diagram, there are only three different propagation velocities for a shock wave:

*free flow*: The propagation velocity of a shock wave in *free flow* is equal to the maximum possible velocity, meaning that the shock wave propagates with exactly the same velocity as the traffic flow, given by:

$$c_{\text{free}} = \left. \frac{dQ}{d\rho} \right|_{\rho < \rho_k} = v_{\max} \quad (18)$$

*congested flow*: On the right side of the fundamental diagram, shock waves propagate with a constant velocity upstream. This velocity is given by the effective vehicle length and the minimum time headway as:

$$c_{\text{cong}} = \left. \frac{dQ}{d\rho} \right|_{\rho > \rho_k} = -\frac{1}{\rho_{\max}T} \quad (19)$$

*free flow*  $\rightarrow$  *congested flow*: The shock wave propagation velocity for transition from *free flow* to *congested flow* is given by the gradient between the corresponding points in the fundamental diagram for vehicle  $i$  and vehicle  $j$ . For  $x_j > x_i$  this means:

$$c_{\text{up}} = \frac{Q_j - Q_i}{\rho_j - \rho_i} = \tilde{c} \quad (20)$$

$c_{\text{up}}$  can take any value between  $c_{\text{cong}}$  and  $v_{\max}$ . As one can easily see in Figure 2, equation 20 is the general solution for the shock wave propagation velocity, labeled by  $\tilde{c}$ .

Knowing the velocities  $v_i$  and  $v_j$  of vehicles  $i$  and  $j$ , respectively, it is possible to estimate the densities  $\rho_i$  and  $\rho_j$  as:

$$\rho_a = \frac{1}{v_aT + \left(\frac{1}{\rho_{\max}}\right)} \quad ; a \in \{i, j\} \quad (21)$$

Again, the idea behind this formula is that every motorist tries to travel with the maximum possible velocity. In our case this means that only the traffic load ahead causes drivers to slow down.

The traffic flows  $Q_i$  and  $Q_j$  can be computed as:

$$Q_a = v_a \rho_a \quad ; a \in \{i, j\} \quad (22)$$

Knowing the velocity, density and flow for two communicating vehicles enables us to gather information about the traffic situation in the intervening space between them.

Our next step is to classify the situation according to the three shock wave propagation possibilities. In case of *free flow* no action needs to be taken, because the traffic flow is propagating downstream with maximum possible velocity. We do not have to take any action if the velocity of the sender is greater than that of the receiver. In the other two cases, an action has to be performed to adapt the velocity of vehicle  $i$  to the conditions given by vehicle  $j$ .

To do so, it is necessary to collect all the needed information. First, the distance between two communicating vehicles, being the range from the tail end of the leading vehicle to the front of the follower, is defined as:

$$d_{i,j} := x_j - x_i - l_{\text{eff}} \quad (23)$$

where  $x_i$  and  $x_j$  are the positions of vehicles  $i$  and  $j$ , respectively.  $l_{\text{eff}}$  is the effective vehicle length. It holds true, that  $l_{\text{eff}} = \frac{1}{\rho_{\max}}$ .

The time gap between the communicating vehicles is given by the formula:

$$\tau = \frac{d_{i,j}}{\Delta v_{i,j}} \quad (24)$$

with  $\Delta v_{i,j} = v_i - v_j$  being the difference of the velocities of vehicle  $i$  and  $j$ . Furthermore, we assume  $v_j \leq v_i$  letting  $v_{i,j}$  always be positive.

By use of equation 20 we can compute the propagation speed of the shock wave within the density gradient between the two vehicles. Knowing that the shock wave travels against traffic flow, the estimated distance between vehicle  $i$  and the tail end of the shock wave, caused by vehicle  $j$ , can be defined as:

$$d_{i,j}^* := d_{i,j} + \tilde{c}\tau \quad (25)$$

Knowing the positions and velocities, as well as an estimate of the shock wave propagation as given in equations 20 and 25, a safe velocity  $v_{i,\text{safe}}$  for the following vehicle  $i$  can be computed as:

$$v_{i,\text{safe}} = v_j + \frac{d_{i,j}^* - v_j T}{\tau} \quad (26)$$

where  $d_{i,j}^*$  is the spatial distance between vehicle  $i$  and the tail end of the shock wave caused by vehicle  $j$ ,  $v_j$  the velocity of vehicle  $j$  and  $\tau$  the time in which vehicle  $i$  will reach vehicle  $j$  with the current velocities  $v_i$  and  $v_j$  as given by equation 24.

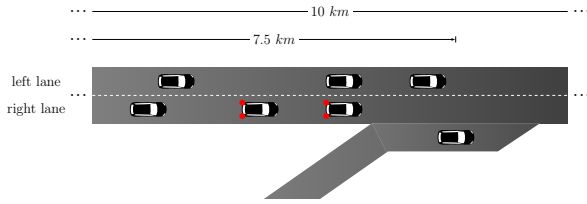


Fig. 3: Simulated road segment

Equation 26 agrees to the velocity computation for the continuous case of the Krauss model [14], [15] extended by an estimation of the shock wave's propagation. For the special case that the distance  $d_{i,j}$  is very small, the propagation of the shock wave is to be neglected, meaning  $d_{i,j}^* = d_{i,j}$ . Hence, equation 26 becomes exactly the velocity formula for the continuous case of the Krauss model.

Another special case is that the velocities of the communicating vehicles are very close together or equal, meaning  $v_i \approx v_j = v$ . Thus leading to a velocity estimate of:

$$v = v + \frac{d_{i,j}^* - vT}{\tau} \quad (27)$$

$$\Rightarrow d_{i,j} + \underbrace{\tilde{c}}_{=0} = vT \quad (28)$$

$$\Rightarrow v = \frac{d_{i,j}}{T} \quad (29)$$

Equation 29 shows that for equal velocities, the maximum safe velocity for vehicles  $i$  and  $j$  is only driven by the distance between the them and the minimum time gap  $T$ .

As the *Kraus* model outputs the maximum safe velocity for a vehicle with respect to the one ahead, one can see that the recommendations by the DRIVE protocol are the maximum velocities to avoid hitting the shockwave downstream in the traffic flow.

In the final step, the anticipated velocity  $v_{i,\text{safe}}$ , given in equation 26, is recommended to the motorist for the duration  $\tau$ , computed by equation 24.

### C. Forward Phase

As our network is operated in multi-hop mode with pure flooding, a receiver should relay each unique message exactly once. Before forwarding, the values for  $x_s$  and  $y_s$  are changed to the relaying vehicles position. Also a new unique message identifier is created by concatenation of the old message identifier and the identifier of the relaying vehicle.

The message forwarding ends if the maximum propagation radius is reached. Since patterns of a wave are recurrent with the wavelength, the maximum message propagation distance has been set to the maximum wavelength of a shock wave, having been determined to be between 1 – 3 km [20].

## V. PROTOCOL EVALUATION

In this section we provide a detailed description of the simulation setup with all the parameters used. We then present a discussion of the simulation results.

### A. Simulation Setup

All traffic simulations in this paper have been performed using SUMO [21]. The access to the running simulation and the inter-vehicular communications have been implemented in

Python with the TraCI interface [22]. The general setup is a two lane highway segment of 10 km with an on-ramp at position 7.5 km as depicted in Figure 3. The total simulation time is 2 hours. Further, we suggest a maximum shock wave wavelength  $\lambda$  of 2000 m, in compliance with the findings in [20]. The traffic model used is the *Krauss car-following model* [14], [15], described earlier in this paper.

The simulations show a common rush-hour scenario with varying inputs on the main lanes and a constant input of 400 vehicles per hour on the on-ramp. Those joining vehicles are responsible for small perturbations on the main lanes in the area of the on-ramp.

To ensure a lifelike mixture of different vehicle types on the simulated road we introduced four different vehicle classes as shown in Table I. Classes A and B represent different kinds of passenger cars. Class A represents the larger motorized class vehicles, while class B stands for the compact. Class C represents small trucks or buses, while class D are the heavy trucks with significantly limited velocity.

During the first 30 minutes of the simulation we considered a moderate traffic flow of 760 vehicles per hour per lane of classes A and B as well as 40 vehicles per hour per lane of classes C and D on the two main lanes. For the next 60 minutes the traffic load on the two main lanes is increased instantaneously to 1,235 vehicles per hour per lane of classes A and B and 65 vehicles per hour per lane of classes C and D. After this peak hour the input is reduced to the initial values for the rest of the simulation. The proportion of 5% to 10% of trucks in overall traffic corresponds to the statistics on vehicle registrations in Europe and the United States [23].

For the communication channel, we suggest a transmission range of 500 m, as defined in the IEEE 802.11p standard [18].

TABLE I: Vehicle classes

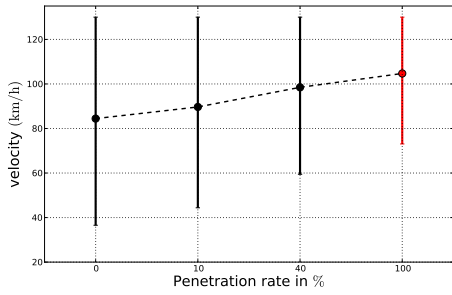
class	$l_{\text{eff}}$ [m]	$a_{\text{max}}$ [m/s <sup>2</sup> ]	$b_{\text{max}}$ [m/s <sup>2</sup> ]	overall %
A	7.5	2.5	-4.5	47.5
B	7.0	1.5	-4.0	47.5
C	17.0	1.2	-4.0	2.5
D	20.0	0.7	-4.0	2.5

### B. Results

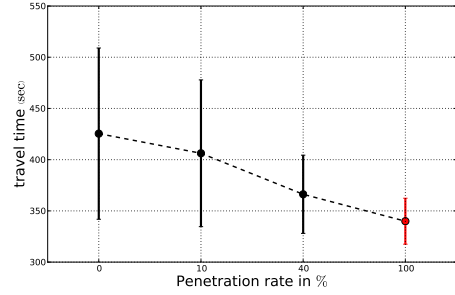
In this section we discuss our simulation results. Two analyses have been performed with different compliance rates to the velocity recommendations computed by the DRIVE protocol. First, we conducted simulations where all the drivers comply to the recommendations of the DRIVE protocol (100% obedience). This study has been made to assess the impact of DRIVE on autonomous or semiautonomous vehicles, which are equipped with systems such as an *Cooperative Adaptive Cruise Control* (CACC). In the second analysis we evaluate the performance of the DRIVE protocol considering human drivers who have to manually adapt the velocity of the vehicle i.e. by the means of a CADAS providing velocity recommendations to the driver. We consider an obedience rate of 75% to take into account the human factor of disobedience towards counterintuitive recommendations of the system. For both studies, different penetration rates of the system have been tested. We compared completely uncoordinated traffic to 10%, 40% and 100% penetration rate of the DRIVE protocol. The simulation results are given in Figures 4, 5 and 6.

Figures 4a and 4b illustrate the mean velocity and the overall travel time with their respective standard deviations

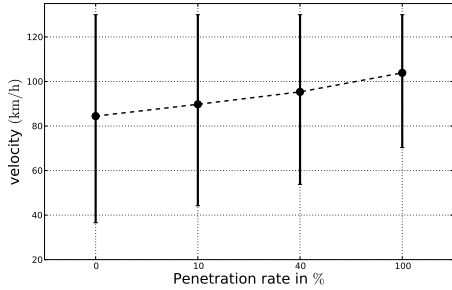




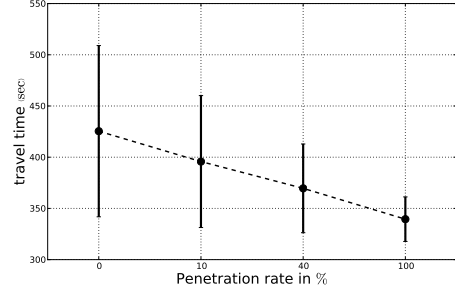
(a) Average velocities with 100% obedience



(b) Overall travel time with 100% obedience



(c) Average velocities with 75% obedience



(d) Overall travel time with 75% obedience

Fig. 4: Statistical evaluation of the average velocities and overall travel time for different penetration rates

for 100% obedience to the recommendations of the DRIVE protocol at different penetration rates. The 100% penetration rate in Figures 4a and 4b, highlighted in red, corresponds to full road coverage with autonomous vehicles. The average velocity can be increased by up to 25%, from  $V_{0\%} = 85$  km/h to  $V_{100\%} = 106$  km/h. Thus the overall travel time is decreased from  $T_{0\%} = 424.4$  s to  $T_{100\%} = 338.3$  s. Even at lower equipment rates DRIVE provides a noticeable improvement of the traffic flow. Already with a penetration rate of only 10%, the overall velocity can be increased by 5% to  $V_{10\%} = 89$  km/h, coincidentally decreasing the overall travel time to  $T_{10\%} = 404.1$  s.

Figures 4c and 4d show the results of the simulation runs with 75% obedience. As mentioned before, those results represent vehicles, still driven manually by humans and reflecting the human imperfections to comply to the recommendations. The results show that the overall velocity can still be increased by up to 25%. This means that a disobedience of 25% of the participating drivers does not significantly affect the performance of DRIVE on the traffic flow.

In addition, the results indicate that even small penetration rates provide noticeable improvements in the overall traffic flow. The fact that the velocities on the road are following a symmetric distribution implies that the standard deviation is a measure of the statistical spread of the velocities. Figure 4 shows that the use of DRIVE makes the spread of velocities and travel times much narrower than within uncoordinated vehicular traffic. This indicates that DRIVE allows reducing the variance of velocity and thus diminishing stop and go traffic.

This finding is further substantiated by Figures 5 and 6.

They depict the time-space charts for simulation runs with uncoordinated traffic flow, and for 10%, 40% and 100% penetration, for 100% and for 75% obedience respectively. Each graph is subdivided into two components, the upper part of each figure shows the left lane and the lower the right lane. The maximum possible velocity at a particular location at a given time is represented by a grey-scale gradient. Whereas Figures 5a and 6a show completely uncoordinated vehicular traffic, Figure 5d illustrates completely coordinated traffic reflecting the upper bound traffic flow improvement using the DRIVE protocol (100% penetration and obedience).

As expected, the graphs for 10% (Figures 5b and 6b) and 40% (Figures 5c and 6c) show that with increasing equipment rate of DRIVE, traffic perturbations are reduced. One can see that in complete accordance with the former results, there are much less stationary or slow moving vehicles on the observed road segment than for the uncoordinated traffic scenario. Again, it becomes clear that even low penetration rates of about 10% improve traffic flow significantly. With increasing penetration rates the formation of traffic jams can be completely eliminated. The improvement of the traffic flow even at low penetration rates can be explained as follows: An equipped vehicle complying to the recommendation of the system will force the following vehicles (even if not equipped) to adjust their own velocity in order to avoid a collision. If this behavior is repeated at several other locations, the formation and propagation of large shock waves can significantly be reduced and as a result, the traffic flow is improved.

## VI. RELATED WORK

Over the last few years, a lot of research has focused on increasing traffic efficiency by exploiting ITS [24]–[26]. The

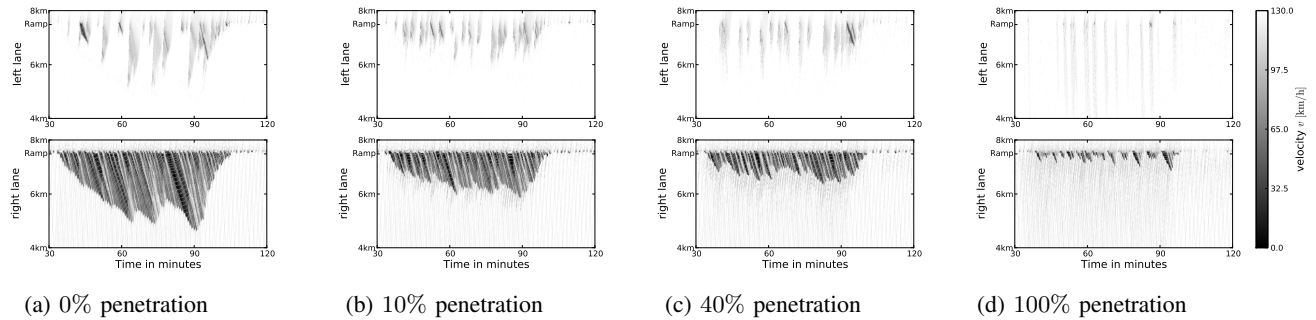


Fig. 5: Velocity over space-time plane with 100% obedience to the recommendations.

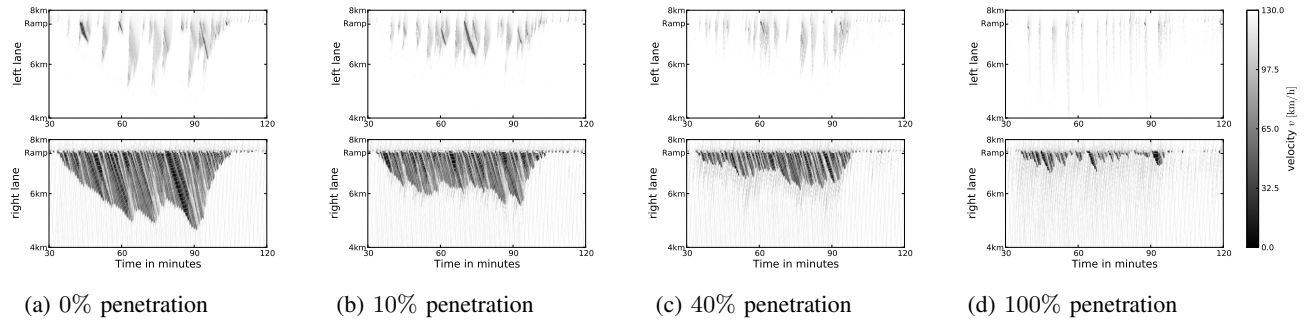


Fig. 6: Velocity over space-time plane with 75% obedience to the recommendations.

following are the most relevant for our work: In [27], the authors have studied the impact of *Variable Speed Limits* (VSL) on highways. Although the primary aim of this study was to increase road safety, they found that using spatially distributed VSL decreases the slope of the flow-density diagram, shown in Figure 2b and shifts the critical occupancy to higher values enabling higher flows at the same traffic density.

In [7], the authors have performed a simulation study to analyze the effect of ACC systems on different traffic scenarios and participation rates. They found that the traffic flows can only be increased at high participation rates if an on-ramp merging scenario is considered. In some cases they found that ACC systems can decrease the overall traffic flow. A similar conclusion has been drawn in [28]. However in the same paper, the authors also studied the impact of a CACC on the flow dynamics. By taking into account one hop inter-vehicular communications, they found that by synchronizing the vehicles, shorter headways can be achieved resulting in increased capacity. A similar approach was proposed in [29], however for different traffic scenarios including capacity reduction. Their results show that the reduced headway leads to the formation of dense platoons, hindering new vehicles to merge with oncoming traffic thus creating more perturbations. They conclude that CACC systems cannot be used to increase traffic flow significantly.

It has been until recently that researchers consider the flow dynamics to increase the efficiency of CACC. In [30], the authors propose a strategy to stabilize traffic flow by periodically broadcasting relevant traffic information to close-by vehicles. Vehicles that detect perturbations downstream try

to keep a larger gap to their predecessor in order to compensate traffic inhomogeneities. They show that at an equipment rate of 30% free flow can be restored even at high traffic densities. An improvement of this work has been proposed by the same authors in [31] where the model includes the effect of the human reaction time, confirming the previous findings.

Our proposal differs from previous works in the following ways: Our protocol is event driven, the procedure is only triggered if a perturbation has been detected. We rely on the LWR model to estimate the current traffic situation and provide optimal recommendation to avoid the formation of shock waves. Finally, we study the impact of difference compliance levels to assess the performance impact of a recommendation based ADAS versus an automated CACC.

## VII. CONCLUSION

In this paper we have introduced DRIVE, a cooperative protocol for *Density Redistribution through Intelligent Velocity Estimation* that propagates traffic information downstream over multiple hops, enabling preventive velocity reductions in order to alleviate the formation of traffic jams caused by shock waves.

The protocol relies on relevant traffic information from vehicles ahead to recommend an optimal velocity in order to prevent traffic perturbations. In practice, such a system could be implemented as a CADAS with communication capabilities to help motorists to adapt their velocity to the current traffic conditions ahead, far beyond the line of sight. Further, such a system can be easily implemented as a CACC to autonomously adapt the velocity.

The simulation results show that DRIVE can significantly



improve the overall traffic situation. We show that on average the velocity can be increased and coincidental overall travel time can be reduced by up to 25% compared to uncoordinated traffic flow. Further, we show that even low equipment rates of 10% are sufficient to achieve significant improvements of the overall traffic flow. This result indicates that even during the roll-out phase of the system an improvement of the traffic situation can be achieved. Finally, by better redistributing the traffic demand, perturbation can be avoided resulting in a more constant traffic flow with less slowdowns thus increasing road safety and comfort and reducing fuel consumption and emissions.

Future work will investigate the possibility of a centralized approach that could be implemented on mobile phones and thus accelerate the time to market of such a system.

#### ACKNOWLEDGEMENT

The authors would like to thank the National Research Fund of Luxembourg (FNR) for providing financial support through the CORE 2010 MOVE project (C10/IS/786097).

#### REFERENCES

- [1] M. Shinkman, M. Buchanan, and E. I. U. G. Britain, *Driving change: how policymakers are using road charging to tackle congestion*. The Economist Intelligence Unit, 2006.
- [2] B. Kerner, *Introduction to Modern Traffic Flow Theory and Control*. Springer Berlin Heidelberg, 2009.
- [3] M. Lighthill and G. Whitham, "On kinematic waves. II. A theory of traffic flow on long crowded roads," *Proceedings of the Royal Society of London. Series A, Mathematical and Physical Sciences*, vol. 229, no. 1178, pp. 317–345, 1955.
- [4] P. Richards, "Shock Waves on the Highway," *Operations research*, vol. 4, no. 1, pp. 42–51, 1956.
- [5] C. J. M. Tampère, S. P. Hoogendoorn, and B. Van Arem, "A Behavioural Approach to Instability, Stop and Go Waves, Wide Jams and Capacity Drop," *Proceedings of the 16th International Symposium on Transportation and Traffic Theory*, pp. 205–228, 2005.
- [6] A. Schadschneider, "Cellular Automaton Approach to Highway Traffic: What do we Know?" pp. 19–34, 2009.
- [7] L. Davis, "Effect of adaptive cruise control systems on mixed traffic flow near an on-ramp," *Physica A: Statistical Mechanics and its Applications*, vol. 379, no. 1, pp. 274 – 290, 2007. [Online]. Available: <http://www.sciencedirect.com/science/article/pii/S0378437106013690>
- [8] K. Nagel and H. J. Herrmann, "Deterministic models for traffic jams," *Physica A Statistical Mechanics and its Applications*, vol. 199, pp. 254–269, Oct. 1993.
- [9] S. and C. Wirasinghe, "Determination of traffic delays from shock-wave analysis," *Transportation Research*, vol. 12, no. 5, pp. 343 – 348, 1978.
- [10] R. Barlovic, L. Santen, A. Schadschneider, and M. Schreckenberg, "Metastable states in cellular automata for traffic flow," *The European Physical Journal B-Condensed Matter and Complex Systems*, vol. 5, no. 3, pp. 793–800, 1998.
- [11] A. Huerre, Patrick and P. Monkewitz, "Local and global instabilities in spatially developing flows," *Annu. Rev. Fluid Mech.*, vol. 22, pp. 473–537, 1990.
- [12] R. E. Wilson, "Mechanisms for spatio-temporal pattern formation in highway traffic models," *Philosophical transactions. Series A, Mathematical, physical, and engineering sciences*, vol. 366, no. 1872, pp. 2017–32, Jun. 2008.
- [13] M. Forster, R. Frank, M. Gerla, and T. Engel, "Improving highway traffic through partial velocity synchronization," in *2012 IEEE Global Communications Conference (GLOBECOM)*, 3-7 December 2012, Anaheim, CA, USA, 2012, pp. 5795–5800.
- [14] S. Krauss, P. Wagner, and C. Gawron, "Metastable states in a microscopic model of traffic flow," *Physical Review E*, vol. 55, no. 304, pp. 55–97, 1997.
- [15] S. Krauß, "Microscopic modeling of traffic flow: Investigation of collision free vehicle dynamics," *Hauptabteilung Mobilität und Systemtechnik des DLR Köln*, no. ISSN 1434-8454, 1998.
- [16] K. Nagel and M. Schreckenberg, "A cellular automaton model for freeway traffic," *Journal de Physique I*, vol. 2, no. 12, pp. 2221–2229, 1992.
- [17] H. Rehborn, S. Klenov, and J. Palmer, "Common Traffic Congestion Features studied in USA, UK, and Germany employing Kerner's Three-Phase Traffic Theory," *ArXiv e-prints*, 2010.
- [18] IEEE, *802.11-2012 - IEEE Standard for Information technology - Telecommunications and information exchange between systems Local and metropolitan area networks - Specific requirements Part 11: Wireless LAN Medium Access Control (MAC) and Physical Layer (PHY) Specifications*. IEEE Computer Society, 2012.
- [19] European Telecommunications Standards Institute, "Intelligent Transport Systems (ITS); Vehicular Communications; Basic Set of Applications; Part 2 : Specification of Cooperative Awareness Basic Service," vol. 1, pp. 1–18, 2011.
- [20] M. Treiber, A. Kesting, and D. Helbing, "Three-phase traffic theory and two-phase models with a fundamental diagram in the light of empirical stylized facts," *ArXiv e-prints*, Apr. 2010.
- [21] M. Behrisch, L. Bieker, J. Erdmann, and D. Krajzewicz, "Sumo - simulation of urban mobility: An overview," in *SIMUL 2011, The Third International Conference on Advances in System Simulation*, Barcelona, Spain, October 2011, pp. 63–68.
- [22] A. Wegener, M. Piórkowski, M. Raya, H. Hellbrück, S. Fischer, and J.-P. Hubaux, "TraCI: an interface for coupling road traffic and network simulators," in *Proceedings of the 11th communications and networking simulation symposium*, ser. CNS '08. New York, NY, USA: ACM, 2008, pp. 155–163.
- [23] UNECE Transport Division, "Road Vehicle Fleet," <http://w3.unece.org/pxweb/dialog/Saveshow.asp?lang=1>, 2013, [March 2013].
- [24] J. Ploeg, B. Scheepers, E. van Nunen, N. Van de Wouw, and H. Nijmeijer, "Design and experimental evaluation of cooperative adaptive cruise control," in *Intelligent Transportation Systems (ITSC), 2011 14th International IEEE Conference on*, 2011, pp. 260–265.
- [25] L. Güvenc, I. Uygan, K. Kahraman, R. Karaahmetoglu, I. Altay, M. Sentürk, M. Emirler, A. Karci, B. Güvenc, E. Altug, M. Turan, O. Tas, E. Bozkurt, U. Özgüner, K. Redmill, A. Kurt, and B. Efendioğlu, "Cooperative adaptive cruise control implementation of team mekar at the grand cooperative driving challenge," *Intelligent Transportation Systems, IEEE Transactions on*, vol. 13, no. 3, pp. 1062–1074, 2012.
- [26] O. Sander, C. Roth, B. Glas, and J. Becker, "Towards design and integration of a vehicle-to-x based adaptive cruise control," in *Proceedings of the FISITA 2012 World Automotive Congress*, ser. Lecture Notes in Electrical Engineering. Springer Berlin Heidelberg, 2013, vol. 200, pp. 87–99. [Online]. Available: [http://dx.doi.org/10.1007/978-3-642-33838-0\\_8](http://dx.doi.org/10.1007/978-3-642-33838-0_8)
- [27] M. Papageorgiou, E. Kosmatopoulos, and I. Papamichail, "Effects of Variable Speed Limits on Motorway Traffic Flow," *Transportation Research Record*, pp. 37–48, 2008.
- [28] J. VanderWerf, S. E. Shladover, M. A. Miller, and N. Kourjanskaia, "Effects of adaptive cruise control systems on highway traffic flow capacity," *Intelligent Transportation Systems and Vehicle-highway Automation 2002: Highway Operations, Capacity, and Traffic Control*, no. 1800, pp. 78–84, 2002.
- [29] B. Van Arem, C. van Driel, and R. Visser, "The impact of cooperative adaptive cruise control on traffic-flow characteristics," *Intelligent Transportation Systems, IEEE Transactions on*, vol. 7, no. 4, pp. 429–436, 2006.
- [30] F. Knorr and M. Schreckenberg, "Influence of inter-vehicle communication on peak hour traffic flow," *Physica A Statistical Mechanics and its Applications*, vol. 391, pp. 2225–2231, Mar. 2012.
- [31] F. Knorr, D. Baselt, M. Schreckenberg, and M. Mauve, "Reducing traffic jams via vanets," *Vehicular Technology, IEEE Transactions on*, vol. 61, no. 8, pp. 3490–3498, 2012.